Received: 03 January 2025 | Revised: 16 May 2025 | Accepted: 02 June 2025

https://doi.org/10.56946/jce.v4i1.604

Journal of Chemistry and Environment

Research Article

Elemental Composition of *Moringa Oleifera Lam* Seeds Using Calibration Free Laser Induced Breakdown Spectroscopy (CF-LIBS)

Abdul Munam Khan*, Irfan Liaquat, Uzma Zahoor*

Department of Physics and Microelectronics, Zhengzhou University, Zhengzhou, China.

*Correspondence:

Uzmazahoor59@gmail.com

Abstract

For centuries, medicinal plants have been widely used to treat numerous diseases. Given the extensive application of *Moringa Oleifera Lam*. in medicine, it is essential to understand its beneficial medicinal properties as well as any potentially toxic elements. In this study, we performed Laser-Induced Breakdown Spectroscopy (LIBS) analysis on *Moringa oleifera* Lam. seeds using a Neodymium-doped Yttrium Aluminium Garnet (ND: YAG) laser in ambient air at varying energies and delay times. Using LIBS, we determined the elemental composition of the seeds and quantified the concentrations of the observed elements via the Calibration-Free (CF)-LIBS technique. The analysis revealed the presence of carbon (C), calcium (Ca), sodium (Na), magnesium (Mg), iron (Fe), potassium (K), aluminium (Al), strontium (Sr), silicon (Si), chromium (Cr), and lithium (Li), along with a molecular CN band. Among these, C, Ca, Na, Mg, Fe, and K were identified as major elements due to their higher concentrations, whereas Sr, Cr, Li, and Al were present in trace amounts. Additionally, we detected a well-defined H-alpha emission line. By analyzing the Stark-broadened line of calcium at 245.38 nm, we estimated the plasma temperature. The electron number density was computed using the Boltzmann plot method based on neutral calcium lines. Finally, we assessed the validity of the Local Thermodynamic Equilibrium (LTE) condition in the plasma.

Keywords: *Moringa Oleifera LAM,* laser induced breakdown spectroscopy, emission spectrum of seeds, local thermodynamic equilibrium.

1. Introduction

Plants are an essential part of the diet for human health and also help to maintain a safe and healthy environment for both humans and animals [1]. Due to a rapid increase in world population, people are cutting down trees. Additionally, forest fires pose a serious threat to plant life. People in even the most remote areas rely on herbal remedies to treat their illnesses [2]. The Moringa tree, scientifically named *Moringa Oleifera LAM*, belongs to the *Moringaceae* family [3]. Common names for this tree include Benzolive, Drumstick, Horseradish, and Moringa [4]. Moringa tree, which is initially in Northern areas of India and along the Himalaya Mountains in Pakistan, now thrives in several regions of Africa, Asia and, South America [5, 6]. In Pakistan, India and Thailand, leaves and fruits of this nutrient-enriched plant are usually used as vegetables and pickles. Due to the significant benefits and nutritional values, most countries now start growing these plants on their own.

Along with their health benefits and enriched with vitamins and nutrition, seeds and leaves have a large biological applications [7]. The World Health Organization (WHO) also recommends Moringa as a healthy food supplement [8]. Several emperors throughout history have utilized the fruits and leaves of the moringa plant to preserve good skin, increase vitality, and ease

tension and pain during battles [7]. According to previous studies, it is found that the *Moringa Oleifera* possesses several noteworthy properties, like anti-asthmatic, anti-oxidant, anti-microbial, anticancer, anti-ulcer, anti-diabetic and anti-hypertensive [9]. Due to the large use of MOLAM in medicine for the treatment of different diseases and to discover the hazardous elements to determine their elemental composition. After analysing, these plants can be used in possible safe and healthy manner.

To utilize the components of *Moringa oleifera Lam* (leaves, seeds, and fruit) for medicinal and dietary purposes, and to explore its broader health benefits, several extraction techniques have been developed. These include supercritical fluid extraction, ultrasound-assisted extraction, pressurized liquid extraction, and microwave-assisted extraction [10]. However, each of these methods presents significant limitations, such as the use of large quantities of hazardous organic solvents, labor-intensive sample preparation, and high operational costs [11]. To overcome these challenges, the elemental composition of *Moringa oleifera Lam* and other medicinal plant extracts can now be effectively determined using Calibration-Free Laser-Induced Breakdown Spectroscopy (CF-LIBS). LIBS, based on atomic emission spectroscopy, is a promising analytical tool that enables both qualitative and quantitative analysis [12]. t is a fast, simple, and versatile technique suitable for multi-element analysis of solids, liquids, gases, metals, and organic samples [13]. Although LIBS is considered a powerful method for in-situ evaluations, detecting trace and hazardous elements in plant matrices remains challenging [14]. Recent studies have applied LIBS to a wide variety of plant materials, including leaves, fruits, seeds, stems, roots, and wood. Gomba et al. [15] uutilized LIBS to determine lithium content in aluminum-lithium alloys, using xenon spectral lines for plasma temperature calculations. LIBS has also been employed in combination with fundamental materials analysis techniques for enhanced results [16].

Furthermore, LIBS has been applied to Indian medicinal herbs to determine carbon, calcium, and magnesium concentrations within the 200–500 nm wavelength range [17]. Jabbar et al. [2] sed laser ablation and spectroscopic analysis to identify elements such as Al, Ba, Mg, Ca, Na, K, O, Sr, H, N, C, Fe, Si, and Cu in the leaves of three medicinal plants—Calotropis procera (apple of Sodom), Chenopodium ambrosioides (Mexican tea), and Nerium indicum (oleander). They found that the essential elements (O, H, C, N), trace elements (Sr, Al, Ba, Si), and medicinally relevant metals (Ca, Fe, Mg, Cu) were present in all samples.. They identified the essential elements O, H, C and N and trace elements Sr, Al, Ba and Si and the required medicinal metals Ca, Fe, Mg and Cu in the leaves of all three plants. By using LIBS investigations Aldakheel, Gondal [18], we can identify the crucial nutrients Mg, Fe, Mn, K, Cu, P, Zn, S, Ca and Na in the spectral lines of *Moringa Oleifera LAM* seeds. To the best of our knowledge, no studies have been carried out on the elemental composition and concentration of both major and trace elements identified in *Moringa Oleifera LAM* seeds. Although several studies have employed LIBS to analyze *Moringa Oleifera LAM* seeds, most have focused on identifying a limited set of elements. However, comprehensive data on both major and trace elemental composition—crucial for assessing medicinal safety and nutritional value—remains scarce. Moreover, a comparative analysis of elemental concentrations under standardized conditions is lacking. This study aims to fill this gap by using LIBS to perform a detailed elemental profiling of *Moringa Oleifera LAM* seeds, ensuring both qualitative and quantitative assessment of essential and potentially hazardous elements.

2. Materials and methods

2.1. Sample preparation

For the experiment, seed samples were collected from the Mirpur district of Azad Jammu and Kashmir (AJK), located at a geographical position of 33° 8' 54.2112" N latitude and 73° 45' 6.3720" E longitude. This region connects to the main Peshawar–Lahore Grand Trunk (GT) Road via Tehsil Dina and is situated at an elevation of approximately 1,560 feet (459 meters) above sea level [19]. Initially, the seeds were thoroughly cleaned and then sun-dried. After drying, the outer coating of the seeds was manually removed. The seeds were then finely ground using a marble mortar and pestle in the laboratory to

obtain a uniform powder. This powdered material was subsequently pressed into pellets using a hydraulic press machine (TMAXCN BATTERY EQUIPMENTS 15T laboratory hydraulic press) for experimental analysis. A total sample weight of approximately 40.64 kg (not 4 tons, as 4 tons equals 4,064 kg—please verify this figure) of *Moringa oleifera Lam* seeds was used in the preparation of the pellets. The seeds and the resulting pellets used for the experimental work are illustrated in figure 1.

Table 1. Details of the sample.

Sample name	Kingdom	Division	Family	Common name
Moringa Oleifera LAM	Plantae	Magnoliophyta	Moringaceae	Sohanjna

2.2. Instrumentation and procedure

The experimental setup used to record the emission spectra of *Moringa oleifera Lam* seeds is illustrated in Figure 2. The system employs a Q-switched Nd:YAG (Neodymium-doped yttrium aluminum garnet) laser (Quanta Ray, LAB SERIES) operating at its fundamental wavelength of 1064 nm, with a pulse duration of 5 ns and an output energy of up to 800 mJ at a repetition rate of 10 Hz. The laser beam is focused onto the target surface using a convex lens with a focal length of 20 cm. The Moringa oleifera sample was placed in ambient air during the experiment. A laser energy meter (Nova-Quantal, France) was used to measure the pulse energy.

To minimize interference from air breakdown in the spectra, the target was positioned precisely at the sharp focus of the lens, at a distance of less than 20 cm. The laser pulse was focused onto the *Moringa oleifera Lam* seed sample to generate sparks, ablate the target surface, and create plasma. To avoid deep cratering and ensure a fresh surface for each laser shot, the sample was mounted on a rotating stage.

Once the high-temperature plasma was generated, the emitted light was collected by a collimating lens and transmitted to the detection system through an optical fiber with high hydroxyl (OH) content and a core diameter of 600 µm.

.

Figure 1. *Moringa Oleifera LAM* seed samples: a) Coated Seeds b) Seeds without outer coat c) Crushed seeds, d) seeds in the form of pellets.

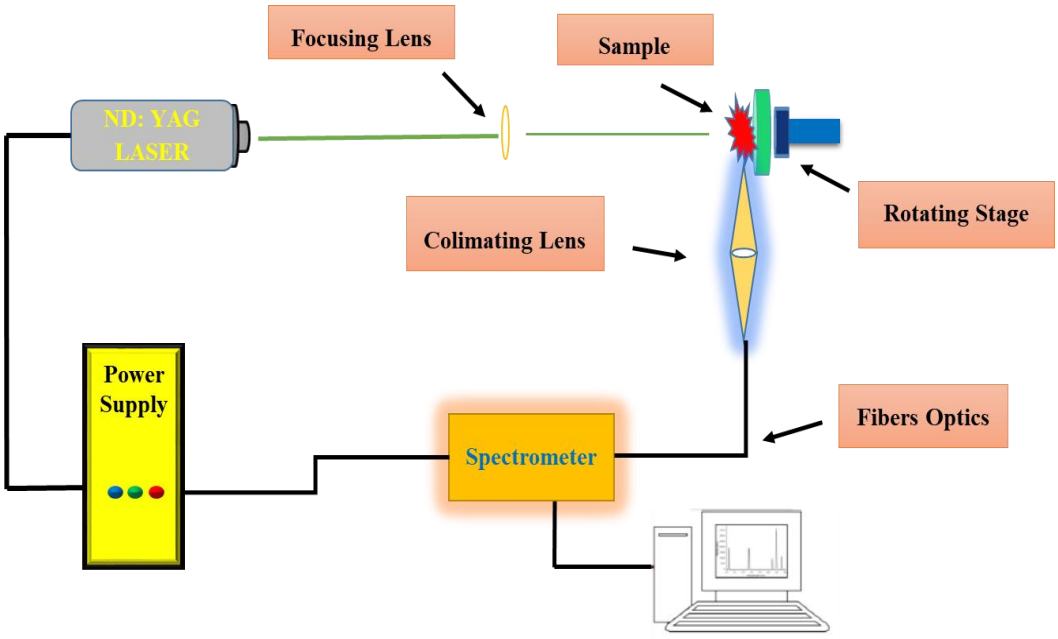

Figure 2. Laser Induced Breakdown Spectroscopy (LIBS) setup.

The detection system comprised a multichannel AVANTES spectrometer (AVS-RACKMOUNT-USB2) featuring a 5 nm slit width and covering a wavelength range from 200 to 950 nm. A narrow-bandwidth dye laser beam, paired with a 2048-element linear charge-coupled device (CCD) array, was employed to evaluate the spectral resolution of each spectrometer channel. The entire detection system was synchronized with the laser pulses via a pulse generator.

The spectrum was recorded with an integration time of 2 milliseconds and a delay time of approximately 2 µs. AVASOFT software was used to simultaneously capture data from all five channels and store it on a PC for further analysis.

3. Results and discussion

3.1. Analysis of emission spectra

The emission spectrum of *Moringa oleifera Lam* (MOLAM) seeds was recorded using a four-level Nd:YAG laser operating at an optimal energy of 65 mJ. The detection system delay time was set to 2 µs. The collimated laser beam was focused onto seed pellets to generate luminous plasma, which contains excited species that emit radiation upon de-excitation. The emitted radiation was captured by the Avantes detection system through an optical fiber. This system includes a spectrometer with a spectral range of 200 to 950 nm. The recorded spectra were saved on a computer using AVO software. Spectral lines were identified based on their wavelengths and intensities, and further verified using the NIST database.

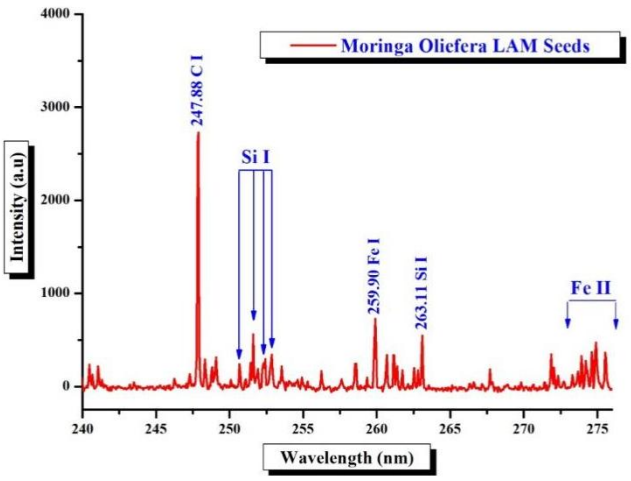

Figure 3. Emission spectrum of *Moringa Oleifera LAM* seeds across the wavelength range of 240 nm to 275 nm.

In Figure 3 (240–275 nm), a strong emission line from neutral carbon is observed at 247.85 nm, corresponding to the $2s^2 2p^2$

$^1P_0 \rightarrow 2s^2 2p^2\ ^1S$ transition. Several neutral silicon lines are detected near 250–253 nm, along with singly ionized iron (Fe II) lines. These findings are consistent with previous LIBS studies on plant materials [20].

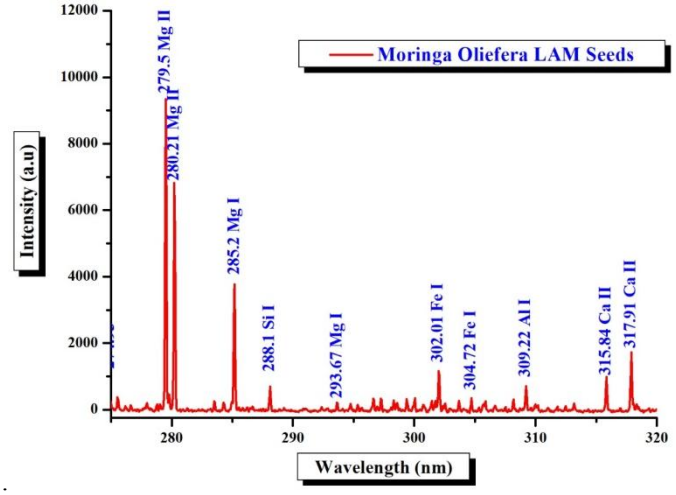

Figure 4. Emission spectrum of *Moringa Oleifera LAM* seeds across the range of 275 nm to 320 nm.

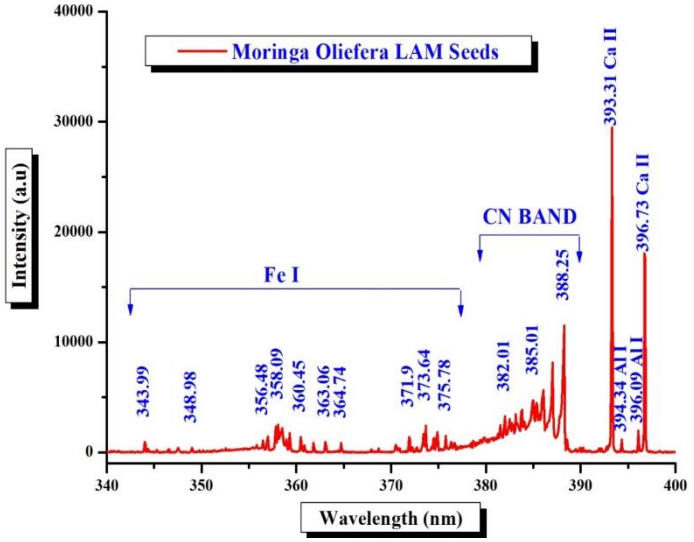

Figure 5. Emission spectrum of *Moringa Oleifera LAM* seeds across the range of 340 nm to 400 nm.

Figure 4 (275–320 nm) presents a detailed spectral profile, highlighting Fe II emission lines at 271.86, 275.52, 283.50, and 284.26 nm. Prominent Mg II doublets at 279.50 nm and 280.21 nm indicate the presence of ionized magnesium, while neutral Mg lines at 277.96 and 285.20 nm further confirm magnesium's presence. Additionally, a silicon emission line at 288.10 nm was detected, affirming the presence of essential nutrient elements. Emission lines corresponding to aluminum and calcium were also observed, consistent with previous LIBS studies on plant materials [21]

In Figure 5 (340–400 nm), multiple Fe I lines ranging from 356.48 to 373.64 nm and Al I lines at 394.34 and 396.10 nm are clearly visible. A distinct molecular CN band is observed between 384 and 390 nm, indicating plasma–air interaction, a common phenomenon under ambient pressure conditions [21]. The presence of CN, N, and O bands signifies molecular recombination events within the plasma.

Figure 6 (400–450 nm) highlights prominent Ca I emissions between 430.15 and 445.38 nm, including the resonance line at 422.60 nm, as well as K I emission at 404.53 nm, both of which are vital for plant physiology. Additionally, Fe I and Fe II lines are observed throughout the spectrum, along with trace amounts of Cr I (427.40 to 438.24 nm) and Sr II at 407.66 and 421.47 nm. The detection of chromium and strontium, both environmentally harmful elements, aligns with previous studies reporting their limited but noteworthy presence in plant materials [21]

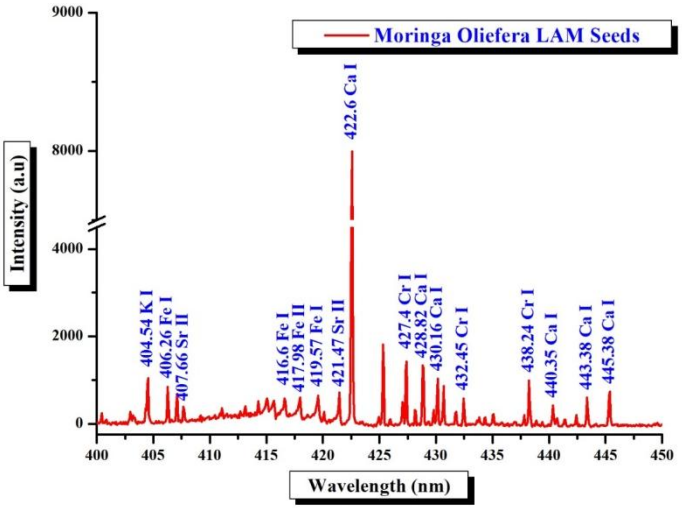

Figure 6. Emission spectrum of *Moringa Oleifera LAM* seeds across the range of 400 nm to 450 nm.

In Figure 7, the laser-induced emission spectra of *Moringa oleifera Lam* seeds are shown within the 580 to 680 nm range. In this region, neutral atomic lines of calcium, sodium, hydrogen, and lithium were detected. Calcium is the dominant element, with prominent emission lines observed at 585.69, 610.23, 612.20, 616.17, 644.69, 646.23, 649.32, and 671.70 nm. A sodium doublet is clearly identified at 588.89 and 589.55 nm. Although sodium is not considered an essential nutrient for

plants, it is beneficial and often used in trace amounts to support metabolic functions. Additionally, a broad hydrogen spectral line is observed at 656.21 nm, exhibiting a strong signal-to-noise ratio, highlighting its physiological relevance despite being a non-mineral element.

In Figure 8 (740–840 nm), a nitrogen triplet appears at 742.46, 744.29, and 746.91 nm, corresponding to transitions from the $3p^4$ P levels to the $3s^4$S states. A potassium doublet is also detected at 766.55 and 769.96 nm, underscoring the presence of this essential macronutrient. Furthermore, a prominent oxygen line at 777.28 nm and neutral carbon emission lines are observed originating from both the seed matrix and its interaction with atmospheric components [22]. Figure 9 (840–915 nm) continues the observed trend, displaying a distinct oxygen emission line at 844.66 nm and several nitrogen emissions ranging from 856.78 to 872.86 nm, corresponding to transitions such as $3p^4D \rightarrow 3s^4P$. Emission lines of singly ionized calcium (Ca II) are identified at 849.74, 854.20, and 866.21 nm, further confirming the earlier detection of calcium in the UV–visible spectral regions. At longer wavelengths, strong carbon emissions are observed at 906.10, 908.82, 909.48, and 911.14 nm, affirming the presence of carbon in the sample with notable intensity [23].

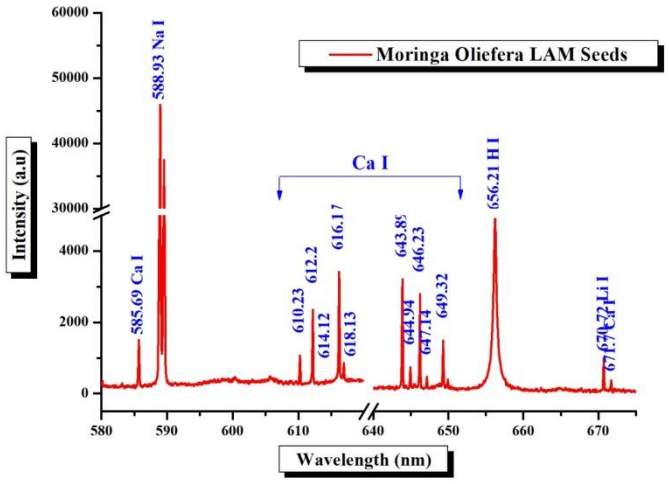

Figure 7. Emission spectrum of *Moringa Oleifera LAM* seeds across the wavelength range of 580 nm to 680 nm.

In the aforementioned Figures 2 to 9, all components detected in *Moringa oleifera Lam* seeds are illustrated. Table 2 lists the main identified elements along with their prominent emission wavelengths. Time-integrated studies demonstrate reliable element identification in the MOLAM seed samples. It has been confirmed that MOLAM seeds contain several elements, including Mg, Fe, Cr, Ca, Na, K, Al, C, Si, Sr, and Li.

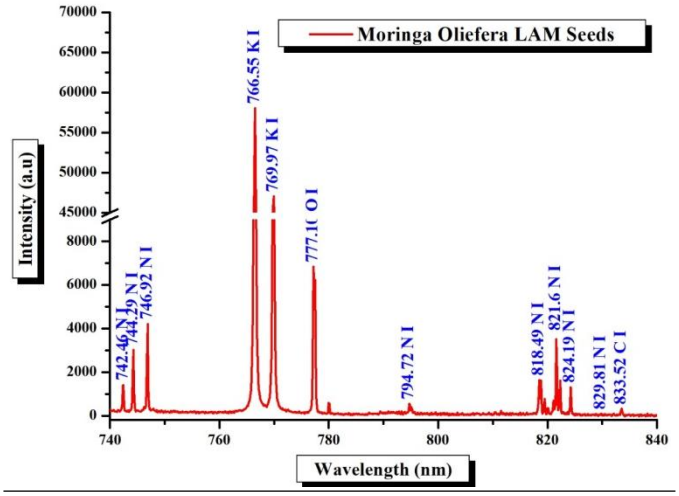

Figure 8. Emission spectrum of *Moringa Oleifera LAM* seeds across the wavelength range of 740 nm to 840 nm.

After identifying all the constituent elements of the sample, the next step is to calculate the weighted elemental concentration for each element. Based on the optical emission spectra of these components, the initial task is to determine the plasma parameters, such as electron number density and plasma temperature.

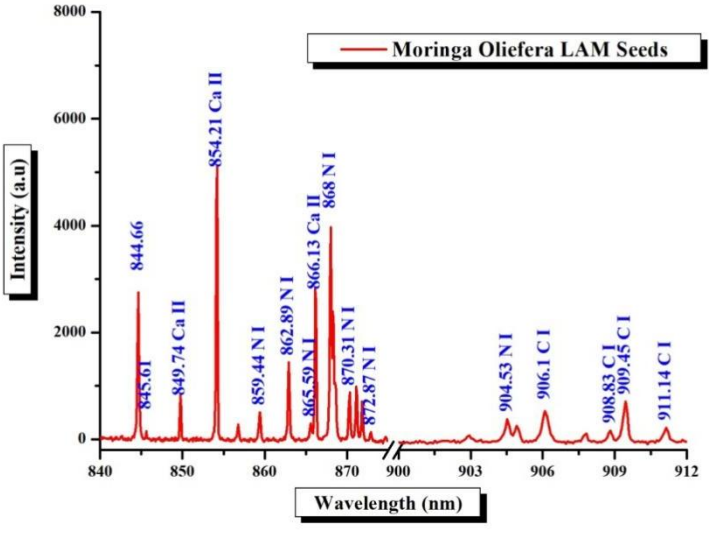

Figure 9. Emission spectrum of *Moringa Oleifera LAM* Seeds across the wavelength range of 580 nm to 680 nm.

3.2. Plasma temperature

When plasma forms on a sample surface, it is essential to understand the processes of atomization, excitation, and

dissociation of the sample. To analyze these plasma-related phenomena, knowledge of the plasma temperature is necessary. Several methods exist for determining the temperature of a plasma generated by an excitation source; among these, the Boltzmann plot method is the most widely used for temperature measurement. The Boltzmann plot method requires optically thin emission lines and a plasma that is spatially and thermodynamically equilibrated [24]. The Boltzmann equation is employed to determine the electron temperature of the plasma produced on the surface of *Moringa oleifera LAM* seeds samples:.

$$\ln\frac{I\lambda}{hcA_{ki}g_k} = -\frac{E_k}{KT} + \ln\frac{CF}{U(T)} \quad \ldots\ldots (1)$$

Where A_{ki} is transition probability, I is the intensity, λ is the wavelength, h (Js) is the plank's constant, c (ms^{-1}) is the speed of light, g_k is statistical weight, E_k (cm^{-1}) is the upper level energy, k (JK^{-1}) is the Boltzmann constant, U (T) is the partition function, and T is plasma temperature. In the present study the neutral calcium lines observed in Moringa*inga oleifera LAM* seeds emission spectra were used to calculate plasma temperature.

Table 2. Wavelengths of main spectral lines identified in *Moringa Oleifera LAM* seeds.

Sample	Element	Main identifying elements (nm)
Moringa	Carbon	247.88, 906.10, 909.45, 911.14
Oleifera	Oxygen	777.10, 844.66
LAM	Hydrogen	656.21
Seeds	Nitrogen	742.46, 744.29, 746.92,794.72, 821.60, 868.00, 870.31, 904.53
	Calcium	393.41, 396.87, 315.91, 317. 97, 422.60, 443.38, 445.38, 610.23, 618.13
	Magnesium	285.22, 382.9, 383.2, 383.8, 516.81 , 517.35, 518.42, 279.07, 279.57, 279.81, 280.28
	Iron	259.96, 273.95 274.74, 337.09, 334.95, 374.96,406.26, 416.60, 438.39
	Chromium	427.4, 432.45, 438.24
	Potassium	766.55, 769.97
	Sodium	588.93, 589.55
	Silicon	250.66, 251.60, 252.42, 288.10
	Lithium	670.72
	Strontium	47.66, 421.47
	Aluminium	308.79, 309.29 ,396.10

Table 3. Ca lines used for Boltzmann plot

Wavelength (nm)	Transition	Statistical weight	Transition probability	Upper-level energy(cm^{-1})
526.57	$3p^6 3d4p\ 3P_1 \rightarrow 3p^6 3d4s\ 3D_2$	3	4.40×10^{07}	39335.32
612.20	$3p^6 4s5s\ 3S_1 \rightarrow 3p^6 4s4p\ 3P_1$	3	2.87×10^{07}	31539.49
649.92	$3p^6 3d4p\ 3F_2 \rightarrow 3p^6 3d4s\ 3D^2$	5	8.10×10^{06}	57730.45
671.76	$3p^6 4s5p\ 1P_1 \rightarrow 3p^6 3d4s\ 1D_2$	3	1.20×10^{07}	36731.61

Table 4. Validity of the McWhirter criteria.

Element	Temperature	Energy difference	Calculated Density	McWhirter Density
Ca I	8000 ± 500 K	2.78239 eV	6.44×10^{16} cm^{-3}	2.53×10^{15} cm^{-3}

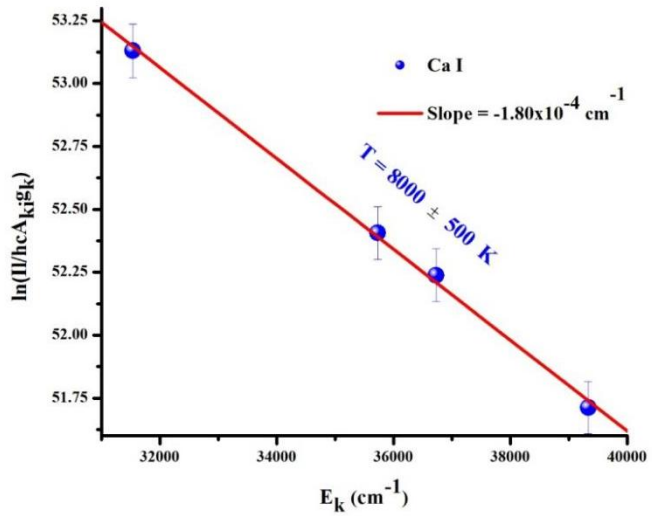

Figure 10. Boltzmann Plot to estimate plasma temperature.

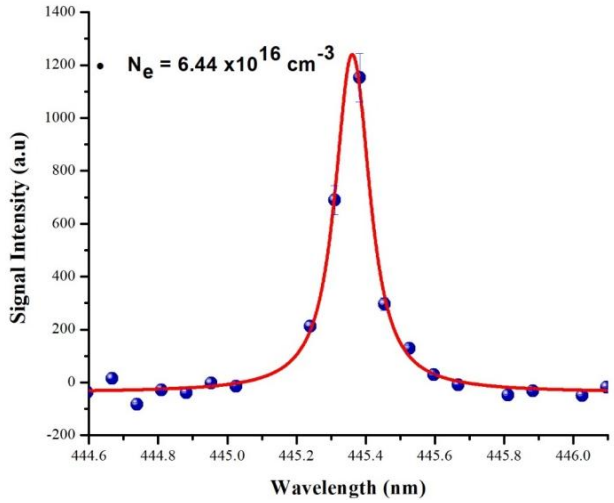

Figure 11. Stark broadened line profile of the Ca I line ($3p^64s4d\ 3D_2 \rightarrow 3p^64s4p\ 3P_2$) at 445.36 nm for the *Moringa Oleifera LAM* seeds. The density was determined as 6.44 x $10^{16} \pm 0.2$ cm^{-3}.

The chosen lines are well-resolved, and there is some uncertainty in the transition probability associated with them. For such transitions, the required spectroscopic data is retrieved from the NIST database [25]. The graph is plotted between the L.H.S of the equation 1 $\left(\ln\frac{I\lambda}{hcA_{ki}g_k}\right)$ taking on y-axis and E_k (Energy of upper level) taken on x-axis. When this figure is linearly fitted, a straight line results. The plasma temperature was calculated using the slope of line. The slop of Boltzmann plot derived from the plot is used to determine the plasma temperature using equation (2).

$$\text{Slope} = -\frac{1}{K_B T} \qquad (2)$$

The data of the neutral calcium lines utilized in the plot are shown in table 3.

The calculated plasma temperature Moringa*inga oleifera LAM seeds* MOSs sample was 8000 K. The typical inaccuracy in the estimated plasma temperature is around 500 K, which is mostly happened due to line intensity measurements and reported transition probabilities.

3.3. Electron number density

The electron density, which is a crucial for defining the plasma's equilibrium state, a significant parameter is used to define the plasma environment. In LIBS, the Stark broadening is used to calculate the electron number density. The spectral line that has been used to calculate the electron number density must be precisely separated and devoid of self-absorption. The neutral line of calcium with transition $3p^64s4d\ ^3D_2 \rightarrow 3p^64s4p\ ^3P_2$ at 445.36 nm is used to compute the density in the present work. By employing the Lorentzian fitting technique along with Stark broadening, we determine the full width at half maximum (FWHM) of the mentioned line of 445.36 nm. This FWHM value is correlated to the electron number density through the equation (3).

$$N_e = \frac{\Delta\lambda_{1/2}}{2\omega} \times N_r \qquad (3)$$

Where $\Delta\lambda_{1/2}$ is FWHM, and is the electron impact parameter at a temperature over 5000 K, obtained from the literature. The value of FWHM is 0.10841 nm and the value of ω is 8.41 x 10^{-3} nm. The Lorentzian fitting of stark broadening is shown in figure 11. Using the values of FWHM and ω I have calculated the electron density 6.44 x $10^{16} \pm 0.2$ cm^{-3}.

The plasma needs to meet the requirements of local thermodynamic equilibrium (LTE) in order to calculate plasma parameters accurately. McWhirter claims that plasma can only be taken into account at LTE when collisional mechanisms predominate the radiative contribution. The McWhirter equation is given as equation (4).

$$N_e \geq 1.6 \times 10^{12} [T(K)]^{1/2} [\Delta E(eV)]^3 \qquad (4)$$

.

Table 5. CF-LIBS composition (% weighted Concentration) of the samples foundMoringa*inga oleifera LAM* seeds.

Element	Neutral Concentration	Ionized Concentration	Total Concentration
C	98.76	11.40	55.08
Ca	0.02	39.01	19.51
Na	0.05	22.45	11.25
Mg	0.26	15.55	7.90
Fe	0.23	7.56	3.89
K	0.002	1.83	0.92
Al	0.02	1.60	0.81
Sr	0.50	0.12	0.31
Cr	0.005	0.39	0.20
Si	0.12	8.2E-06	0.06
Li	0.0001	0.05	0.02

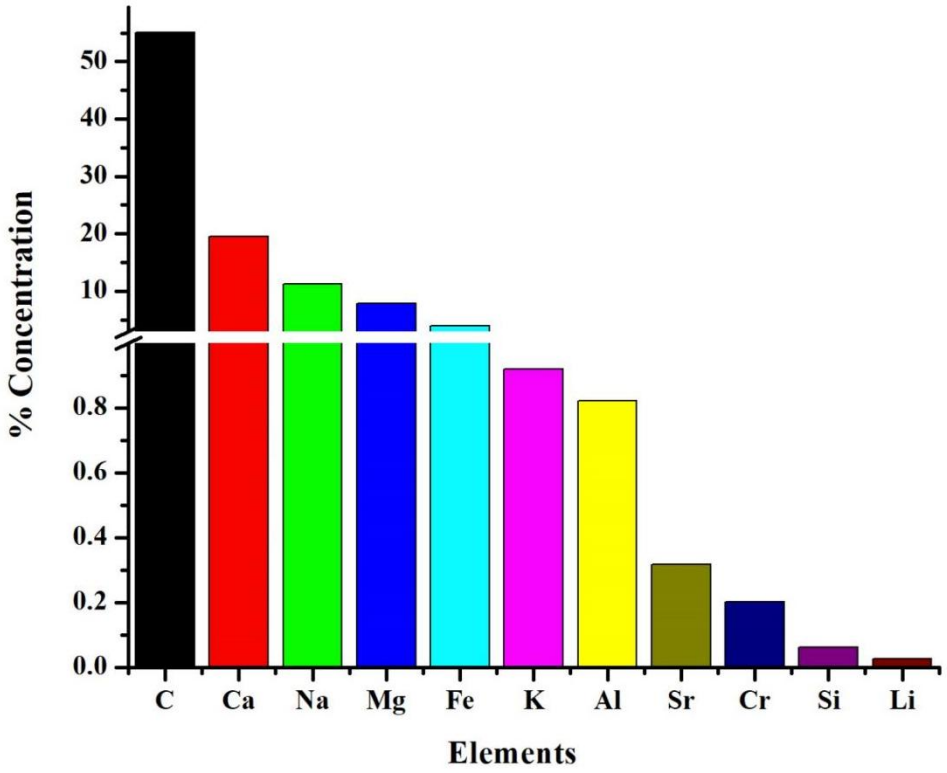

Figure 12. Bar graph showing the determined elemental concentrations by CF-LIBS

By putting the values of temperature and difference of energy between the lower and upper levels of calcium 445.36 nm, we determined the value of density 2.5350×10^{15} cm^{-3} which is significantly smaller than the calculated density from the Stark broadened line of Ca at 445.36 nm. This shows that the local thermodynamic equilibrium condition for this plasma analysis is fulfilled. Table 4 provides the plasma temperature, energy difference, and computed electron density for the LTE

validity check.

3.4. Compositional analysis by CF-LIBS

Once the local thermodynamic equilibrium (LTE) conditions are met and the plasma temperature and electron plasma density are determined, a crucial step is to compute the elemental concentration of our sample based on experimental data. A method known as Calibration-free (CF) Laser-Induced Breakdown Spectroscopy (LIBS), pioneered by Ciucci, Corsi [26] enables quantitative elemental analysis using LIBS spectra. In the current study, we applied the CF-LIBS method to determine the concentration of elements in *Moringa Oleifera LAM* seeds.

This technique relies on optically thin lines and the fulfillment of LTE within the plasma [27].

Here is the Boltzmann equation, which establishes a relationship between the intensities of emission lines originating from the same species.

$$FC_Z = I_k \frac{U^Z(T)}{A_{ki} g_k} exp^{(\frac{Ek}{kT})} \quad (5)$$

Here, F represents the experimental factor, which remains constant when the spectral efficiency of the system is constant. Z denotes the partition functions, which were computed in this study using the NIST database and the calculated temperature of 0.68938 eV. Uz (T) represents the concentration of the neutral species. I_k refers to the intensity of the emission line, A_{ki} is the transition probability, and g_k represents the statistical weight, Ek stands for the upper-level energy, K is the Boltzmann constant, and T denotes the plasma temperature determined via the Boltzmann Plot method.

We employed the following equation to determine the concentration of neutral species:

$$C_z = \frac{U_z(T)}{F} Exp\ (Q_s) \quad (6)$$

Where,

$$Q_s = ln\left(\frac{I\lambda}{hcA_k g_k}\right) + \frac{E_k}{K_B T} \quad (7)$$

For the measurement of concentration of the ionic species we have used the following equation:

$$n_e \frac{C_z+1}{C_z} = \frac{(2\pi mKT)^{3/2}}{h^3} \frac{2U^{z+1}(T)}{U^z(T)} \exp\left(\frac{-E_{ion}}{KT}\right) cm^{-3} \quad (8)$$

The ionization energy of the spectral species is denoted by E_{ion}, while m_e represents the mass of the electron, and h stands for Planck's constant. All other parameters in Equation 8 have their standard values. The total concentration of both neutral and ionized species can be computed using the following relation:

$$C^s = C_z + C_{z+1} \quad (9)$$

The concentrations of ionized and neutral species are represented by C_{Z+1} and $C_{Z,}$ respectively. The percentage concentration can be determined using the following relation:

$$C^s{}_{\%} = \frac{C^s \times W^s}{(\sum_{s=1}^{n} C^s \times W^s)} \times 100 \quad (10)$$

The concentration of a single element is denoted by C^s %, where W^s represents the atomic weight, and S= 1, 2, 3…, signifies the element's number. This equation allowed us to ascertain the composition of all elements in the MOSs sample. Notably, Nitrogen and Oxygen were excluded from the compositions due to limitations of our spectrometer. The elements along with their percentage concentrations, are listed in Table 5.

We have identified 12 elements in Moringa*inga oleifera LAM* seeds sample. In our analysis, the major elements included carbon (C), sodium (Na), calcium (Ca), iron and magnesium (Mg). Additionally, there were minor elements with significantly lower concentrations, namely potassium (K), aluminium (Al), strontium (Sr), chromium (Cr), silicon (Si), and lithium (Li).I have calculated the concentration of C (55.08%), Ca (19.51%), Na (11.25%), Mg (7.90%), Fe (3.89%), K (0.92%), Al (0.81%), Sr (0.31%), Cr (0.20 %), Si (0.06%), and Li (0.02%). A comparison of the percentage concentrations of identified elements in Mor*inga oleifera LAM* seeds (MOSs) is shown in figure 12.

4. Conclusion

This study employed Laser-Induced Breakdown Spectroscopy (LIBS) to analyze the elemental composition and plasma parameters of Moringa oleifera LAM seeds (MOSs) using a Nd:YAG laser in ambient air. The Calibration-Free LIBS (CF-LIBS) technique effectively identified major elements such as C, Ca, Na, Mg, Fe, and K in higher concentrations, along with trace elements including Sr, Cr, Li, Al, and Si. The detection of the CN molecular band and the H-alpha emission line

further indicated the complexity of the seed matrix. Plasma characterization revealed an electron number density of 6.44×10^{16} cm^{-3} and a plasma temperature of 8000 ± 500, validated under Local Thermodynamic Equilibrium (LTE) conditions. The findings highlight the potential of Moringa oleifera seeds in the formulation of dietary supplements, functional foods, and phytopharmaceutical products. Moreover, LIBS demonstrates significant advantages as a rapid, cost-effective, and non-destructive technique for elemental analysis, offering promising applications in quality control within the food, herbal, and nutraceutical industries. Its adaptability for large-scale industrial analysis and regulatory compliance makes LIBS a valuable tool in modern analytical methodologies.

Authors Contribution

Abdul Munam Khan: Conceptualization, Data curation, Investigation, Methodology, writing original draft; Irfan Liaquat visualization, Review, editing; Uzma Zahoor: Resources, Review, Supervision.

Conflicts of Interest

There are no conflicts of interest reported by the writers.

Funding Not applicable (N/A)

Acknowledgment

Success of this project depends largely on the encouragement efforts, determination, and contribution of all authors.

Data Availability statement

The data presented in this study are available on request from the corresponding author.

REFERENCES

1. Kiritkar, K. and B. Basu, Indian Medicinal Plants. Blatter E, Caicus, JF and Mhaskar KS. International Book Distributors, Dehradun, 1999. 1: p. 545-546.
2. Jabbar, A., et al., Analytical approach of laser-induced breakdown spectroscopy to detect elemental profile of medicinal plants leaves. Indonesian Journal of Chemistry, 2019. 19(2): p. 430-440.
3. Khor, K.Z., et al., The in vitro and in vivo anticancer properties of Moringa oleifera. Evidence-Based Complementary and Alternative Medicine, 2018. 2018.
4. Agrawal, T., ETHNOBOTANY OF PROSOPIS CINERARIA. 2017.
5. Al-Zahrani, A.A. and A.H. Ibrahim, Changes in 2S albumin gene expression in Moringa oleifera under drought stress and expected allergenic reactivity in silico analysis. Theoretical and Experimental Plant Physiology, 2018. 30(1): p. 19-27.
6. Gandji, K., et al., Status and utilisation of Moringa oleifera Lam: A review. African Crop Science Journal, 2018. 26(1): p. 137-156.
7. Yalew, T.A., Y. Mekonnen, and N. Retta, Comparison of total phenolic content, free radical scavenging potential and antihyperglycemic condition from leaves extract of Moringa stenopetala and Moringa oleifera. Ethio. J. Pub. Health Nutr, 2019. 1: p. 20-27.
8. Lin, M., J. Zhang, and X. Chen, Bioactive flavonoidsMoringainga oleifera and their health-promoting properties. Journal of functional foods, 2018. 47: p. 469-479.
9. Rode, S.B., et al., Nature's gold (Moringa oleifera): miracle properties. Cureus, 2022. 14(7).
10. Zhong, J., et al., The application of ultrasound and microwave to increase oil extraction fMoringainga oleifera seeds. Industrial Crops and Products, 2018. 120: p. 1-10.
11. Belo, Y.N., et al., Ultrahigh-pressure supercritical fluid extraction and chromatography of Moringa oleifera and Moringa peregrina seed lipids. Analytical and bioanalytical chemistry, 2019. 411(16): p. 3685-3693.
12. Cremers, D.A., et al., Laser-induced breakdown spectroscopy, elemental analysis. Encyclopedia of Analytical Chemistry: Applications, Theory and Instrumentation, 2006.
13. Visentini, U., et al., Accurate measurement of magnesium content in alpha-olefins by laser induced

breakdown spectroscopy (LIBS) technique. Optoelectronics Letters, 2007. 3(3): p. 222-226.

14. Kaiser, J., et al., Trace elemental analysis by laser-induced breakdown spectroscopy—Biological applications. Surface Science Reports, 2012. 67(11-12): p. 233-243.
15. Gomba, J., et al., Spectroscopic characterization of laser induced breakdown in aluminium–lithium alloy samples for quantitative determination of traces. Spectrochimica Acta Part B: Atomic Spectroscopy, 2001. 56(6): p. 695-705.
16. Jabbar, A., et al., On the detection of heavy elements in the Euphorbia indica plant using laser-induced breakdown spectroscopy and laser ablation time of flight mass spectrometry. Journal of Analytical Atomic Spectrometry, 2019. 34(5): p. 954-962.
17. Rai, P.K., et al., Use of laser-induced breakdown spectroscopy for the detection of glycemic elements in Indian medicinal plants. Evidence-Based Complementary and Alternative Medicine, 2013. 2013.
18. Aldakheel, R., et al., Spectral analysis of Miracle Moringa tree leaves using X-ray photoelectron, laser induced breakdown and inductively coupled plasma-optical emission spectroscopic techniques. Talanta, 2020. 217: p. 121062.
19. Rafique, M., Cesium-137 activity concentrations in soil and brick samples of Mirpur, Azad Kashmir; Pakistan. International Journal of Radiation Research, 2014. 12(1): p. 39.
20. Molina M, J., et al., Assessing the Sensitivity and Efficiency of Laser-Induced Breakdown Spectroscopy (LIBS) for High-Concentration Cadmium Detection in Cocoa Powder. Sensors, 2025. 25(8): p. 2434.
21. Kamil, Z.J., M.J. Zoory, and H.J. Mohamad, LIBS technique for plant mineral ratio analysis and environmental and agricultural importance: a comprehensive review. The European Physical Journal D, 2024. 78(3): p. 27.
22. Maharaj-Sharma, R., Solar Variability of the Atomic Oxygen O (1S) Greenline Emissions in the Middle and Lower Thermosphere. 2003: National Library of Canada= Bibliothè que nationale du Canada, Ottawa.
23. Shamsipur, M., A. Barati, and S. Karami, Long-wavelength, multicolor, and white-light emitting carbon-based dots: Achievements made, challenges remaining, and applications. Carbon, 2017. 124: p. 429-472.
24. Le Drogoff, B., et al., Temporal characterization of femtosecond laser pulses induced plasma for spectrochemical analysis of aluminum alloys. Spectrochimica acta part B: Atomic spectroscopy, 2001. 56(6): p. 987-1002.
25. Jabbar, A., et al., Elemental analysis of plants cultivated in saline soil by laser-induced breakdown spectroscopy (LIBS). Analytical Letters, 2021. 54(8): p. 1351-1365.
26. Ciucci, A., et al., New procedure for quantitative elemental analysis by laser-induced plasma spectroscopy. Applied spectroscopy, 1999. 53(8): p. 960-964.
27. Corsi, M., et al., Double pulse, calibration-free laser-induced breakdown spectroscopy: a new technique for in situ standard-less analysis of polluted soils. Applied Geochemistry, 2006. 21(5): p. 748-755.

How to cite this article:
Khan A.M., Liaquat I., Zahoor U. (2025). Elemental Composition of *Moringa oleifera Lam* Seeds Using Calibration-Free Laser-Induced Breakdown Spectroscopy (CF-LIBS). Journal of Chemistry and Environment, 4(1), p. 81–92.